Enhancing cancer therapeutics using size-optimized magnetic fluid hyperthermia

Amit P. Khandhar, R. Matthew Ferguson, Julian A. Simon, and Kannan M. Krishnan

Citation: J. Appl. Phys. **111**, 07B306 (2012); doi: 10.1063/1.3671427
View online: http://dx.doi.org/10.1063/1.3671427
View Table of Contents: http://jap.aip.org/resource/1/JAPIAU/v111/i7
Published by the American Institute of Physics.

Enhancing cancer therapeutics using size-optimized magnetic fluid hyperthermia

Amit P. Khandhar,[1] R. Matthew Ferguson,[1] Julian A. Simon,[2] and Kannan M. Krishnan[1,a)]
[1]*University of Washington, Materials Science & Engineering, Seattle, Washington 98195, USA*
[2]*Fred Hutchinson Cancer Research Center, Division of Clinical Research, Seattle, Washington 91809, USA*

(Presented 3 November 2011; received 22 September 2011; accepted 18 October 2011; published online 13 February 2012)

Magnetic fluid hyperthermia (MFH) employs heat dissipation from magnetic nanoparticles to elicit a therapeutic outcome in tumor sites, which results in either cell death (>42 °C) or damage (<42 °C) depending on the localized rise in temperature. We investigated the therapeutic effect of MFH in immortalized T lymphocyte (Jurkat) cells using monodisperse magnetite (Fe_3O_4) nanoparticles (MNPs) synthesized in organic solvents and subsequently transferred to aqueous phase using a biocompatible amphiphilic polymer. Monodisperse MNPs, ~16 nm diameter, show maximum heating efficiency, or specific loss power (watts/g Fe_3O_4) in a 373 kHz alternating magnetic field. Our *in vitro* results, for 15 min of heating, show that only 40% of cells survive for a relatively low dose (490 μg Fe/ml) of these size-optimized MNPs, compared to 80% and 90% survival fraction for 12 and 13 nm MNPs at 600 μg Fe/ml. The significant decrease in cell viability due to MNP-induced hyperthermia from only size-optimized nanoparticles demonstrates the central idea of tailoring size for a specific frequency in order to intrinsically improve the therapeutic potency of MFH by optimizing both dose and time of application. © *2012 American Institute of Physics*.
[doi:10.1063/1.3671427]

I. INTRODUCTION

Hyperthermia, heating disease sites to 42–45 °C to cause cell damage or death, is a promising mode of adjuvant cancer therapy intended to enhance the efficacy of traditional therapies such as radiotherapy and chemotherapy.[1] The synergistic effect of hyperthermia has been studied in both cell cultures and animal models.[2–4] However, clinical adoption of hyperthermia faces limitations such as the challenge of restricting the heating to only the tumor sites[5] and the reduced effectiveness of heating due to the development of thermal tolerance in cells from expression of heat shock proteins.[6] Blood flow at tumor sites is highly irregular and also poses several challenges, but there is evidence to suggest that hyperthermia can be effective if significant localized heating is achieved.[7] Magnetic fluid hyperthermia (MFH) offers a promising approach for localized hyperthermia.[8–11] It requires delivering magnetic nanoparticles (MNPs) at the tumor site and applying a well-defined alternating magnetic field (AMF). MNPs dissipate heat in an applied AMF due to power losses resulting from lagging particle magnetizations. Detailed mathematical treatments describing the origins of these power losses are well established and can be found elsewhere.[12,13]

For safe application of MFH, superparamagnetic magnetite (Fe_3O_4) MNPs dispersed in water with biocompatible polymers are most suitable since they are widely used in biomedical studies.[10,11,14] Furthermore, compared to ferromagnetic metal or alloy MNPs,[15,16] superparamagnetic Fe_3O_4 MNPs have modest magnetic characteristics and require utmost optimization of morphological (size, size distribution, shape), crystallographic (phase purity), and magnetic (relaxation) characteristics for effective application in MFH.[17] For optimization of the power loss (P), and attain maximum heat dissipation, it is important to tailor the material parameters of MNP for the specified AMF frequency, f and amplitude, H_0. This is given by Eq. (1),[18]

$$P = \pi\mu_o H_o^2 \chi'' f \int_0^\infty g(R)dR, \tag{1}$$

where μ_o is the permeability of free space ($4\pi \times 10–7$ H/m), $g(R)$ is the lognormal size distribution of a dispersion of MNPs having radii R, and χ'' is the out-of-phase susceptibility given by

$$\chi''(\omega) = \chi_o \frac{2\pi f\tau}{1+(2\pi f\tau)^2}, \tag{2}$$

where χ_o is the DC-susceptibility and τ is the effective relaxation time of the particles given by the Brownian (τ_B) and Néel (τ_N) components, both material parameters that depend on the hydrodynamic diameter and magnetic core diameter, respectively. In a previous study,[19] we experimentally showed that the material parameter, τ, is optimized by synthesizing monodisperse Fe_3O_4 MNPs of various sizes and plotting the specific loss power, or the power dissipated per unit mass of MNPs (SLP, watts/g Fe_3O_4), as a function of core size. Our results showed that 16 nm diameter was the optimum diameter in an applied AMF of $f = 373$ kHz and $H_0 = 14$ kA/m. Furthermore, these experimental results were compared with a rigorously developed theoretical model by Carrey *et al.*[13] According to this model, the optimum volume (V_{opt}) for randomly oriented MNPs is given by

a)Author to whom correspondence should be addressed. Electronic mail: kannanmk@uw.edu.

$$V_{opt} = \frac{-k_B T \ln(\pi f \tau_0)}{K_{eff}\left(1 - \frac{1.69\mu_0 H_{\max} M_s}{2K_{eff}}\right)^{\frac{4}{3}}}, \quad (3)$$

where k_B = Boltzmann constant (1.38×10^{-23} J K^{-1}), T = temperature (300 K), f = applied field frequency (kHz), τ_0 = attempt time ($\sim 10^{-10}$ s), K_{eff} = anisotropy constant (23–41 kJ m^{-3}),[18] $\mu_0 H_{\max}$ = field amplitude ($4\pi \times 10^{-7}$ H m^{-1} * $H_{\max}$ kA m^{-1}), and M_s = saturation magnetization (450 kA m^{-1}).[20] Depending on the anisotropy constant of magnetite, for an AMF with $f = 373$ kHz and $H_{\max} = 14$ kA m^{-1}, the optimum diameter ($D_{opt} = [6*V_{opt}/\pi]^{1/3}$) can range from 13 nm (for $K_{eff} = 40$ kJ m^{-3}) to 17 nm (for $K_{eff} = 23$ kJ m^{-3}). This confirms that our experimental results, which indicate 16 nm as the peak diameter, fall within the range predicted by the theoretical model.

MFH has been studied extensively in both *in vitro*[21–24] and *in vivo*[25–27] platforms. However, most studies in MFH investigate "extrinsic" augmentations in order to counteract the ineffectiveness of polydisperse MNP dispersions to improve therapeutic efficiency. We have intrinsically optimized MFH by tailoring the size and size distribution of MNPs, resulting in maximum SLP output for our chosen AMF conditions ($f = 373$ kHz and $H_0 = 14$ kA/m). Furthermore, we show the direct consequence of such optimization on viability of cancer cell populations by testing the *in vitro* efficacy of MFH.

II. EXPERIMENTAL METHODS

A. Synthesis of monodisperse water-stable magnetite (Fe_3O_4) MNPs

Organic synthesis routes offer exceptional control over MNP size and size distribution, which is unmatched by aqueous synthesis routes.[28,29] The synthesis method used in this study is based on pyrolysis of the Fe^{3+}-oleate precursor. The ratio of precursor to surfactant (oleic acid) determines the final core size of Fe_3O_4 MNPs. For example, using a precursor to surfactant of 1:15 resulted in highly monodisperse 15 nm MNPs. After transfer from organic to aqueous phase using poly(maleic anhydride-alt-1-octadecene)-poly(ethylene glycol) (PMAO-PEG), an amphiphilic polymer, the final solution (MNP@PMAO-PEG) was a stable colloid dispersion of Fe_3O_4 MNPs in de-ionized (DI) water. MNP concentration was typically 2–4 mg MNP/ml and determined using Inductively Couple Plasma Atomic Emission Spectrophotometer (ICP-AES, Jarrell Ash 955). Nanoparticles were analyzed using transmission electron microscope (TEM - FEI Tecnai^{TM} G2 F20) images to gain a visual perspective and confirm the overall uniformity in the iron oxide core diameter and its distribution. However, due to the finite viewing area in a TEM image, statistically significant size analysis is not possible. As a result, magnetization curves of liquid samples (containing 100–200 μg MNPs), measured by VSM, were fit to the Langevin function to obtain the magnetic core diameter and distribution. Further details of the experimental procedure and size characterization results are reported elsewhere.[17,19]

B. Colloidal stability in cell culture medium

We have shown previously[19] that the SLP deteriorates significantly due to reduced Brownian relaxation when MNPs agglomerate in biological medium. As a result, prior to *in vitro* experiments, hydrodynamic size measurements in biological medium [RPMI 1640 + 10% fetal bovine serum (FBS)] were done at several time points using a dynamic light scattering (DLS) instrument (Zetasizer Nano, Malvern instruments).

C. *In vitro* magnetic fluid hyperthermia (MFH)

Jurkat cells were grown in RPMI 1640 medium + 10% FBS in physiological conditions (37 °C and 5% CO2). Cells were cultured in triplicates at a density of 10 000 cells/well. MNPs of three diameters (12 nm; $\sigma = 0.09$, 13 nm; $\sigma = 0.22$ and 16 nm; $\sigma = 0.16$)[30] with varying concentrations were mixed in growth medium with cells. Jurkats are suspension cells and can interact with MNPs also suspended in medium; however, Jurkats are not known to uptake or bind MNPs. As a result, MNP relaxation is expected to be similar to that in growth medium.

Prior to heating in an AMF ($f = 373$ kHz and $H_0 = 14$ kA/m), samples (cells + MNPs + MFH) and controls (cells + MNPs − MFH and cells-MNPs-MFH) were incubated at 37 °C for 15 mins to stabilize temperature. Cell vials were enclosed in a thermally insulating Styrofoam^{TM} jacket before inserting in the coil assembly of the hyperthermia instrument (nanoTherics, magneTherm, UK). Temperature was measured using a sensitive fiber optic thermocouple (Luxtron, Lumasense Technologies). After 15 mins of AMF application, cells were returned to the 37 °C incubator for 15 mins. Samples and controls were allowed to equilibrate with room temperature for 30 mins prior to viability measurements using the Celltiter-GLO® luciferase assay (Promega). The luciferase assay is a viability assay (% live cells) and measures ATP levels, or the number of metabolically active cells.

III. RESULTS AND DISCUSSION

A. Colloidal stability in biological medium

MNPs preferentially disperse in the aqueous phase after coating with PMAO-PEG and show no signs of agglomeration for several months (Fig. 1(a), data shown for 1 month). Hydrodynamic size measurements in RPMI 1640 + 10% FBS medium confirm MNP@PMAO-PEG are stable and do not agglomerate over time (Fig. 1(b), data shown for 4 h). Colloidal stability in growth medium ensures minimal loss in SLP during the course of the experiment. It should be noted that serum in cell culture medium consists of numerous proteins and antibodies that have a significant contribution to the MNP hydrodynamic size. This explains the sharp peak at smaller diameters in the number distribution is from the medium and does not indicate MNPs become smaller.

B. *In vitro* hyperthermia

Typical heating curves of 12, 13, and 16 nm (diameter) MNPs in DI water, normalized for MNP concentration, are

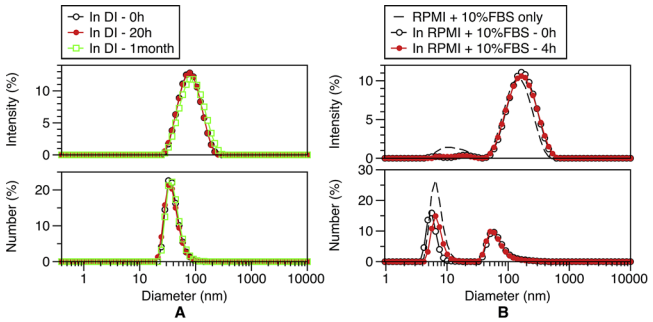

FIG. 1. (Color online) (a) Hydrodynamic size of MNPs in DI water as intensity (%) and number (%) distributions. MNPs are stable for several months (data only shown till 1 month). (b) Intensity (%) and number (%) size distributions of MNP@PMAO-PEG in RPMI 1640 + 10% FBS cell culture medium as a function of time. The growth medium has a significant contribution to the hydrodynamic size, which is distinctly visible in the number distribution. MNPs are stable in RPMI + 10% FBS for several hours.

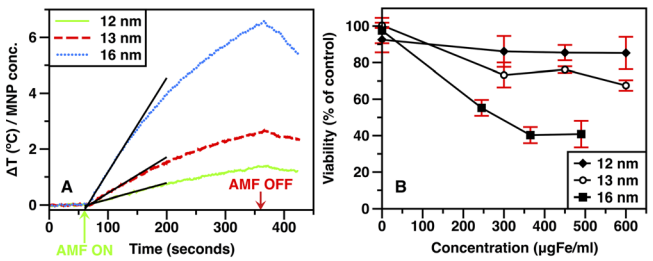

FIG. 2. (Color online) (a) Normalized heating curves of 12, 13, and 16 nm MNPs in DI water. Slope (dT/dt) of the initial curve (70–130 s) was normalized for Fe_3O_4 concentration and used to determine the SLP. For $f = 373$ kHz and $H_0 = 14$ kA/m, 16 nm monodisperse MNPs show maximum SLP. (b) 16 nm MNPs result in 60% decrease in viability of Jurkat cells, compared to 5% and 25% decrease when 12 and 13 nm MNPs are used, respectively.

shown in Fig. 2(a). The background temperature was measured for 60 s, followed by 300 s of heating in the AMF. The initial linear slope (dT/dt) from 70 to 130 s was normalized for Fe_3O_4 concentration and used to determine the SLP. The heating curves confirm our previous results that 16 nm is the optimum diameter for an AMF operating at 373 kHz and 14 kA/m, and shows maximum rise in temperature during the period when AMF is turned on (60–360 s).

Figure 2(b) shows the *in vitro* effect of MFH on the viability of Jurkat cells. As expected, increasing concentration of all MNP sizes results in a decrease in cell viability. However, the viability decrease as a function of size is more significant and underlines the true effect of size-optimized MFH. Hyperthermia induced by the optimum 16 nm MNPs results in ~60% decrease of cell viability (relative to control) at 490 μgFe/ml,[31] compared to ~25% decrease by 13 nm MNPs at 600 μgFe/ml and only ~5% decrease by 12 nm MNPs, also at 600 μgFe/ml.

IV. CONCLUSIONS

We have shown that 16 nm is the optimum diameter and shows maximum heating rate for our field conditions ($f = 373$ kHz and $H_0 = 14$ kA/m) and translates truthfully to cell populations as long as colloidal stability, and thus relaxation dynamics, of MNPs is preserved in biological medium. Cell viability of Jurkat cells decreased by ~60% when MFH was induced by 16 nm MNPs at 490 μgFe/ml, compared to ~5% and ~25% decrease when induced by 12 and 13 nm MNPs at 600 μgFe/ml, respectively.

Use of sub-optimal MNPs for MFH results in several challenges and exacerbates clinical adoption. In the past, researchers have implemented extrinsic enhancements such as significantly increasing MNP concentration, or using high amplitude fields. Clinical applications, however, limit such extrinsic enhancements due to the maximum tolerable dose of both MNPs and field intensity. Ferromagnetic nanoparticles with significantly high SLP values than magnetite have also been proposed, but due to the high risks to biological systems, clinical adoption of materials other than magnetite is highly unlikely or requires extensive regulatory verification. Conversely, synthesizing monodisperse magnetite MNPs with sizes tailored for a given AMF frequency fundamentally optimizes MFH and shows great promise in validating MFH as a promising adjuvant therapy in cancer.

ACKNOWLEDGMENTS

This work was supported by NIH/NIBIB R21 EB008192 and NIH/NIBIB RO1 EB013689.

[1]G. M. Hahn, IEEE Trans. Biomed. Eng. **31**, 3 (1984).
[2]K. J. Henle and D. B. Leeper, Radiat. Res. **66**, 505 (1976).
[3]J. B. Marmor, Cancer Res. **39**, 2269 (1979).
[4]B. Hildebrandt *et al.*, Cr. Rev. Oncol-Hem. **43**, 33 (2002).
[5]R. Hergt and S. Dutz, J. Magn. Magn. Mater. **311**, 187 (2007).
[6]S. Lindquist and E. A. Craig, Annu. Rev. Genet. **22**, 631 (1988).
[7]C. W. Song, Cancer Res. **44**, 4721s (1984).
[8]M. Yanase *et al.*, Cancer Sci. **89**, 775 (1998).
[9]A. Jordan *et al.*, J. Magn. Magn. Mater. **201**, 413 (1999).
[10]Q. A. Pankhurst *et al.*, J. Phys. D: Appl. Phys. **42**, 22401 (2009).
[11]K. M. Krishnan, IEEE Trans. on Magn. **46**, 2523 (2010).
[12]R. Hergt *et al.*, IEEE Trans. on Magn. **34**, 3745 (1998).
[13]J. Carrey *et al.*, J. Appl. Phys. **109**, 083921 (2011).
[14]A. K. Gupta and M. Gupta, Biomaterials **26**, 3995 (2005).
[15]Y. Bao and K. M. Krishnan, J. Magn. Magn. Mater. **293**, 15 (2005).
[16]Y. Bao, H. Calderon, and K. M. Krishnan, J. Phys. Chem. **C111**, 1941 (2007).
[17]A. P. Khandhar *et al.*, "Tailored magnetic nanoparticles for optimizing magnetic fluid hyperthermia," J. Biomed. Mater. Res. A (in press).
[18]R. E. Rosensweig, J. Magn. Magn. Mater. **252**, 370 (2002).
[19]A. P. Khandhar, R. M. Ferguson, and K. M. Krishnan, J. Appl. Phys. **109**, 07B310 (2011).
[20]R. M. Cornell and U. Schwertmann, *The Iron Oxides: Structures, Properties, Reactions, Occurrence and Uses* (Weinheimm, New York, 1996).
[21]J.-P. Fortin *et al.*, Eur. Biophys. J. **37**, 223 (2008).
[22]I. Hilger *et al.*, Nanotechnology **15**, 1027 (2004).
[23]A. Jordan *et al.*, J. Magn. Magn. Mater. **194**, 185 (1999).
[24]C.-h. Hou, Biomaterials **30**, 4700 (2009).
[25]I. Hilger *et al.*, IEE P-Nanobiotechnol. **152**, 33 (2005).
[26]R. Ivkov *et al.*, Clin. Cancer. Res. **11**, 7093s (2005).
[27]M. Kawashita *et al.*, Biomaterials **26**, 2231 (2005).
[28]N. R. Jana *et al.*, Chem. Mater. **16**, 3931 (2004).
[29]Hyeon *et al.*, J. Am. Chem. Soc. **123**, 12798 (2001).
[30]MNP sizes are median core diameters determined by fitting magnetization curves to the Langevin function. MNPs are assumed to follow a lognormal distribution and σ is the standard deviation of the lognormal distribution function.
[31]Due to technical problems with the ICP-AES, the concentration of 16 nm MNPs was rechecked and, in fact, found to be lower than 12 and 13 nm MNPs.